Finite-Difference Modeling of Fractured Media

Reeshidev Bansal* and Mrinal K. Sen
Institute for Geophysics, John A. and Katherine G. Jackson School
of Geosciences, University of Texas at Austin

Summary

We propose modeling of fractured reservoirs based on equivalent media theory. A 3D fnite-differnce scheme was developed to simulate wave propogation in arbitrary anisotropic media. The anisotropic media upto orthorhombic symmetry using Standard Staggered Grid scheme (SSG) and beyond (monoclinic and triclinic) were modeled using Rotated Staggered Grid scheme (RSG). Observation of the horizontal component seismogram confirms the fact the S-wave data alone cannot distinguish between gas- and fluid-filled fractures.

Equivalent Media Theory

In seismic frequency band, closely spaced parallel fractures behave like an anisotropic medium. A number of equivalent media theories were proposed in the last two decades. The most general and accurate equivalent media theories were proposed by Hudson (1980) and Schoenberg (1980) for penny-shaped cracks and planar discontinuities (fractures), respectively. Even though both the approaches are completely different, they result in the same equivalent elastic coecients for cracks and fractures. This observation suggests that the shape of the fractures cannot be uniquely resolved by seismic methods. The equivalent elastic coe cients are expressed in terms of fracture parameters such as fracture orientation, fracture or crack density and fracture in fill (gas or fluid).

Finite-Difference Modeling in Anisotropic Media

Numerical modeling of wave propagation is an important tool for both earthquake- and exploration-seismologists.

It has been used for forward modeling in the inverse problems to support the interpretation of seismic data and to understand the wave propagation in complex media. There are a number of techniques to simulate wave propagation numerically, and a comprehensive review can be found in Carcione et al. (2002). Finite-di”erence scheme, even though computationally expensive compared to other schemes, most accurately simulates the wave propagation because it directly solves the wave-equation. Hence, this scheme accounts not only for the direct waves, re ected waves, multiply reflected waves, but also for surface waves, head waves, and waves in ray-shadow zone (Kelly et al., 1976).

Finite-difference scheme can be implemented either by velocity-stress formulation or by displacement-stress formulation (Virieux, 1984). Here, we implement the velocity-stress formulation to simulate the wave propagation in anisotropic media.

Basic Numerical Procedure

Equation of motion is given as (Aki and Richards, 2002)

$$\rho u_{t} = \sigma ij,j + f_{i} \qquad (1)$$

and constitutive relationship for general anisotropic media can be written as

$$\sigma ij,j = C_{ij}kluk,l, \qquad (2)$$

where *ui* is the particle displacement, σi is the stress tensor, fi is the body force per unit volume, and *cijkl* summarizes the elastic properties of the medium. Equations 1 and 2 are linear first-order coupled equations for particle displacement or velocity, and stress. Taking first time derivative of equation 2 and substituting velocity of the particle for displacement in equation 1, we obtain a first-order system of equations in velocity and stress which can be solved numerically. Standard Staggered Grid (SSG) Finite-Difference Scheme

To implement finite-difference scheme, all the quantities (cijkl, ρ, σij, *ui*) in equations 1 and 2 need to be discretized.

Virieux (1984) first described a standard way of discretization of these quantities in a staggered grid (figure 1(a)).

The main advantage of using the staggered grid is that the spatial derivatives are calculated at half the grid

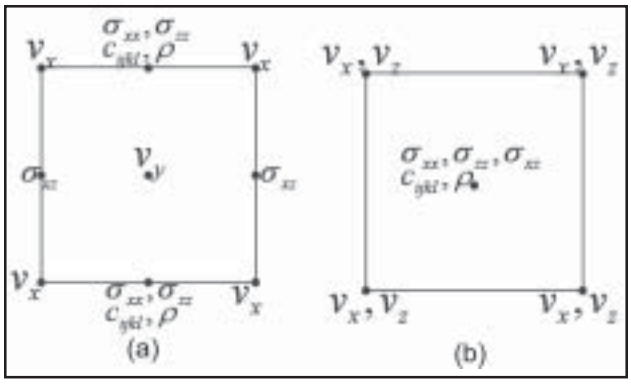

Fig. 1: (a) Elementary cell of standard staggered grid: Notice that σxz is not defined at the location of stiffness tensor c_{ijkl}. Density ρ of the medium is also not defined at the location where particle velocities vx and vz are defined. This necessitates the interpolation of the cijkl and ρ. (b) Elementary cell of rotated staggered grid: Notice that all the components of the stress are defined at the same location. Hence, no interpolation of the stiffness tensor c_{ijkl} is needed. But the density ρ of the medium still needs to be interpolated to estimate the particle velocities vx and vz.

points. It should be noted that grid size is an important parameter in finite-diffrence scheme. Large grid size allows for computation of large models, but very large grid size tends to push the numerical dispersion in the computation outof acceptable limits (e.g., Marfurt, 1984). Furthermore, small grid size requires small time-steps to avoid numerical instability, which will increase the computation time.

In the staggered grid discretization (figure 1(a)), some coefficients of the elastic stiffness matrix c_{ijkl} and density ρ need to be interpolated to compute the off-diagonal stress components (in 2D that is σ_{xz}, and in 3D those are σ_{yz}, σ_{xy}, σ_{xy}) and the particle velocities, respectively. Moreover, if the medium posses the symmetry lower than orthorhombic, which is the case if the medium has two sets of non-orthogonal fracture sets, some components of the strain or particle velocities need to be interpolated to compute the Hook sum (equation 2).

To test the accuracy of this method, wave propagation was simulated in a large model of HTI media (figure 2(a)). The elastic constants of the medium are as follows (the factor of 10^9 N/m^2 is omitted): c_{11}= 15:0, c_{33}=30.0, c_{13} = 4.0, c_{44} = 8.0, and c_{55}= 4.0. The density of the medium is 2000 kg/m^3

The model has 450 grid points with equal grid spacing of 10 m in all the directions. An explosive source is placed at the center of the model. The source wavelet is a Gaussian with a dominant frequency of 15 hz. A snapshot in 3D at 400 ms after the explosion is shown in figure 2(a).

Rotated Staggered Grid (RSG) Finite-Di"erence Scheme As mentioned earlier, in case of medium symmetry lower than orthorhombic, standard staggered grid discretization turns out to be error prone. To calculate the synthetic section in monoclinic or triclinic media a better grid discretization is needed. The straightforward solution seems to be defining all components of stress at one grid location and all components of the particle velocity at the next grid location. But this scheme will require huge computer memory and longer computation time to run a realistic model. To circumvent this problem, another discretization scheme in a rotated staggered grid was proposed by Gold et al. (1997). Here, for the sake of simplicity, discretization is explained in 2D. The medium is divided into rectangular or square grids or cells. All the particle velocities are defined at the nodes of the cell. All the components of stress, strain and medium properties (c_{ijkl} and ρ) are defined at the center of the cell (figure 1(b)). Now, either the elastodynamic equations 1 and 2 can be rotated along the diagonals of the cell and spatial derivatives of velocities and stress components can be calculated at the appropriate grid locations, or spatial derivatives can be first calculated along diagonals of the cells and then transformed back along the edges of the cells. It turns out that the algebra involved is not very complicated in the second approach, and hence, it can be implemented numerically with ease (e.g., Saenger et al., 2000).

We implemented this scheme in 3D for general anisotropic media with 21 independent elastic constants. To test the robustness and stability of this method in general anisotropic media, wave propagation in a large model of a homogeneous triclinic medium was simulated. An explosion source is kept at the center of the model. The dominant frequency of the Ricker wavelet is 15 hz. Figure 2(b) shows a snapshot of wave propagation in 3D at 400 ms after explosion. All three types of waves (qP, qS1, and qS2) can be identified.

Modeling Examples

To test the accuracy of the modeling algorithms and to simulate the fracture response in surface seismic data, a number of 3D shotgathers were generated for various subsurface models. Both explosive source and plane-wave shear source were used to generate these seismic sections.

A typical three at-layered subsurface model (Figure 3) was used to generate all the seismic sections. Although the finite-difference algorithms are capable of handling subsurface models with complex geometry, at-layered

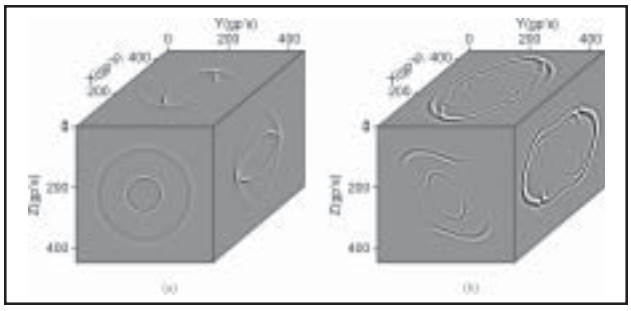

Fig.2: A snapshot (x-velocity) after 400 time steps (400 ms) in: (a) HTI medium. The model is a homogeneous block with 450 grid points (grid spacing 10 m) in all the directions. Both P-, SV-waves can be observed. Notice the triplication in SV-wave in yz-and xy-plane ; (b) triclinic medium. All three types of wave qP1, qS1, and qS2 can be identified.

models were used to study the fracture response in the seismic data. Top and bottom layers are isotropic, and the middle layer has one set of vertical parallel fractures. Background P-wave and S-wave velocities α, β and density ρ in each layer are: 2.5 km/s, 1.4 km/s and 1 g/cm^3 ; 3.5 km/s, 2.0 km/s and 2.3 g/cm^3 ; 4.5 km/s, 3.0 km/s and 3.5 g/cm^3 .There are 141 and 86 geophones at the interval of 10 meters in x- and y-direction, respectively. For convenience, lines along x-and y-axes will be called x-line and y-line, respectively. The shot is at the middle of y-axis. The near-offset is 150 meters in x-direction. The survey layout remains the same for all the seismic experiments.

Fractures density e in the middle layer is 0.05; fractures can be either gas- or water-filled, and are striking in y-direction (fracture normal is parallel to x-direction). ΔN and ΔT are used to estimate the equivalent stiffness matrix for the middle layer (see Bakulin et al., 2000 for details). Table 1 summarizes all the relevant parameters for the Figure

Table 1: Notice that ΔT remains same for gas- and water-filled fractures. Thus, c_{44} and c_{55} of stiffess matrix remains samefor gas- and water-filled fractures which implies that vertical S-wave velocities $S^{\parallel}$ and $S^{\perp}$in both the cases also remain the same.

Relevant parameters of the middle layer in subsurface model (Figure 3)						
Filling fage	α	β	ρ	e	Δ_N	Δ_T
Gas	3.5 km/s	2.0 km/s	2.3 g/cm^3	0.05	0.303	0.113
Water	3.5 km/s	2.0 km/s	2.3 g/cm^3	0.05	0.0	0.113

4 shows an x-line at y-location 20 meter from the shot generated using an explosive source when the middle layer has gas-filled fractures. A Gaussian wavelet with dominant frequency of 15 hz was used as source function. Although all three velocity components vx, vy and vz were recorded, only vx (figure 4(a)) and vy (figure 4(b)) are displayed to observe the S-wave splitting due to presence of the fractures in the middle layer. Reflection about 1.5 s is the converted

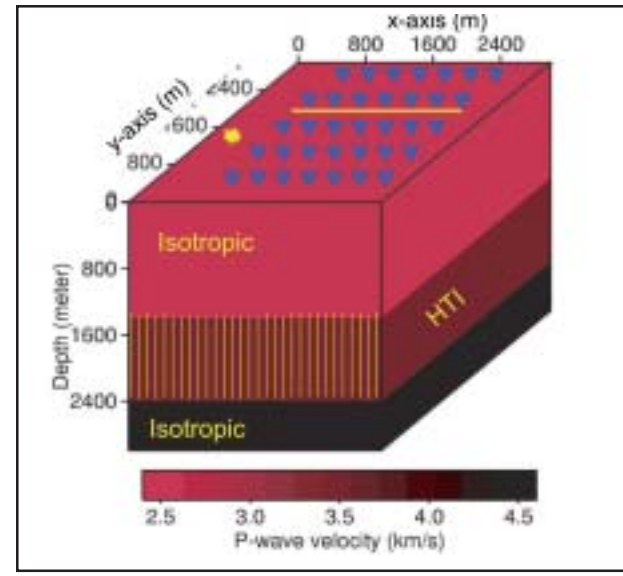

Fig. 3: This is the three at-layered subsurface model used to generate shot gathers. Middle layer has one set of vertical fractures striking in y-direction (fracture normal is parallel to x-direction). Crack or fracture density e is 0.05

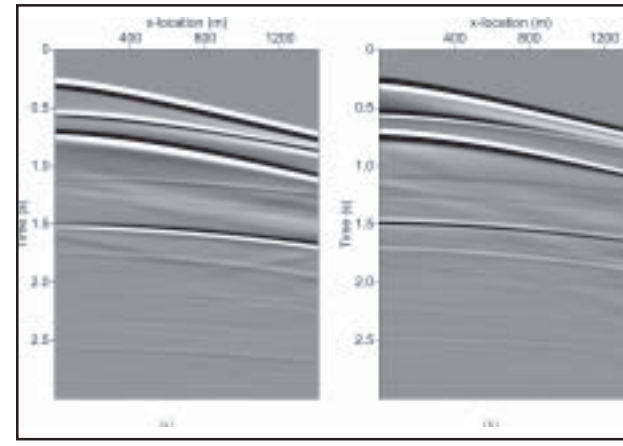

Fig.4 : Shotgathers using an explosive source: (a) x-component of velocity vx, (b) y-component of velocity vy. Notice the time-difference at near-offset in the arrivals at 1.5 s in both the sections. This time-di”erence is attributed to the presence of vertical fractures in the middle layer (figure 3). Finite-Difference Modeling middle layer. Relevant parameters of the middle layer in subsurface model (Figure 3)

S-wave from the interface between middle layer and bottom layer. Notice the time-difference between vx and vy arrivals at near-offset at 1.5 s; vx arrivals are polarized normal to fracture strike and vy arrivals are polarized parallel to fracture strike. Thus, vx are traveling slower than vy.

Above experiment was simulated with a plane-wave shear source. The particle motion is polarized linearly at 45 clockwise from x-axis; i.e., vx and vy are excited in phase

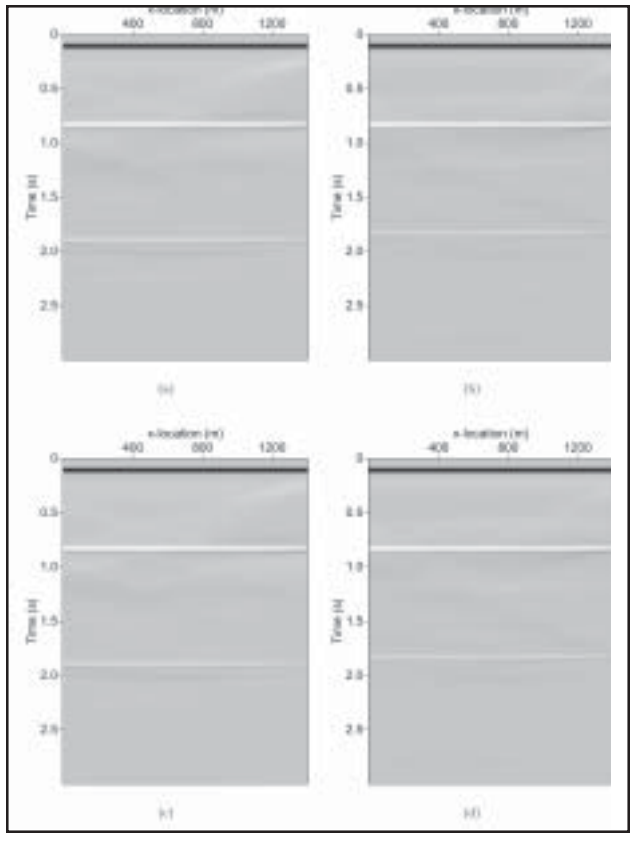

Fig.5: Seismic sections using a plane-wave source. (a) x-component of velocity vx for gas-filled fractures, (b) y-component of velocity vy for gas-filled fractures, (c) x-component of velocity vx for water-filled fractures, (d) y-component of velocity vy for water-filled fractures. Notice the time-di"erence in the arrivals about 1.8 s between vx and vy sections. It is same for gas- and water-filled fractures because vertical S-wave velocities ($S^{||}$ and $S^{\perp}$) are the same in both the cases.

with equal amplitudes. Figure 5 shows the vx and vy for both gas-filled (Figures 5(a) and 5(b)) and water-filled (Figures 5(c) and 5(d)) fractures. Notice the time-di"erences between vx and vy arrivals for both the cases; they appear to be same. This is due to the fact that constants c44 and c55 in stiffness matrix remain same for gas- and water-filled fractures, which eventually leads to same vertical S-wave velocities ($S^{||}$ and $S^{\perp}$) in both the cases. This observation suggests that stacked S-wave sections are unable to reveal the fracture-infill (gas or water) in the subsurface. Hence, some other techniques (e.g., AVO analysis, P-wave NMO analysis, S-wave NMO-analysis) need to be applied to fully characterize fractures in the subsurface.

Discussion and Future Work

So far, we have shown the results only from at layers. We are planning to simulate the wave propagation in more complex models to understand the combined e"ect of anisotropy and complex structures.

References

Aki, K., and Richards, P. G., 2002, Quantitative seismology: University Science Books.

Bakulin, A., Grechka, V., and Tsvankin, I., 2000a, Estimation of fracture parameters from re ection seismic data{part I: HTI model due to a single fracture set: Geophysics, 65, no. 6, 1788 - 1802.

Carcione, J. M., Herman, G. C., and ten Kroode, A. P., 2002, Seismic modeling: Geophysics, 67, no. 4, 1304{1325.

Gold, N., Shapiro, S. A., and Burr, E., 1997, Modelling of high contrasts in elastic media using a modified finite difference scheme:, in 67th Ann. Internat. Mtg Soc. of Expl. Geophys., 1850-1853.

Hudson, J. A., 1980, Overall properties of a cracked solid: Math. Proc. Camb. Phil. Soc., 88, 371- 384.

Kelly, K. R., Ward, R. W., Treitel, S., and Alford, R. M., 1976, Synthetic seismograms: a finite-difference approach: Geophysics, 41, 2{27.

Marfurt, K. J., 1984, Accuracy of ˇnite-di"erence and ˇnite-element modeling of the scalar and elastic wave equations: Geophysics, 49, no. 5, 533{549.

Saenger, E. H., Gold, N., and Shapiro, S. A., 2000, Modeling the propagation of elastic waves using a modified definite-difference grid: Wave Motion, 31, 77{92.

Schoenberg, M., 1980, Elastic wave behavior across linear slip interfaces: J. Acoust. Soc. Am., 68, 1516{1521.

Virieux, J., 1984, SH-wave propagation in heterogeneous media: Velocity-stress finite-diffrence method: Geophysics, 49, no. 11, 1933{1957.